Calculation of Space-Charge Forces in the Analysis of Traveling-Wave Tubes

H. K. Detweiler

Telecommunications Division

A comprehensive large-signal traveling-wave tube computer program has been developed for the study and design optimization of high-efficiency space-type tubes. Studies have been made previously with a theory which employs a "deformable-disk model" (DDM) for the electron beam, but neglects RF space-charge forces in the beam. That theory was found to yield accurate predictions for tubes in which RF space-charge forces are not the predominant factor in determining device performance. However, RF space-charge effects can be very important in tubes designed for space flight applications. Thus, it is essential to include them in the computer calculations if accurate predictions of device performance are to be obtained. Expressions for the space-charge fields, appropriate to the DDM representation of the electron beam, are presented in this article and the methods used in the calculations are described.

Introduction

A comprehensive large-signal traveling-wave tube (TWT) computer program has been developed for the study and design optimization of high-efficiency space-type tubes. This program allows for a consideration of the various magnetic focusing means which are commonly employed to minimize weight and has provisions for determining the efficacy of the phase-focusing techniques used to improve efficiency.

A typical TWT configuration is schematically illustrated in Figure 1. In essence, this device consists of an electron gun, an RF circuit capable of supporting the propagation of a slow electromagnetic wave having a longitudinal electric field component, and an electron collector. Electrons are emitted from the cathode and focused into a beam in the gun region such that their motion is predominantly parallel to the axis of the slow-wave circuit. They next traverse the circuit region where an interaction takes place with the RF wave propagating on the circuit. Subsequently, the electrons enter the collector and are removed from the device. When

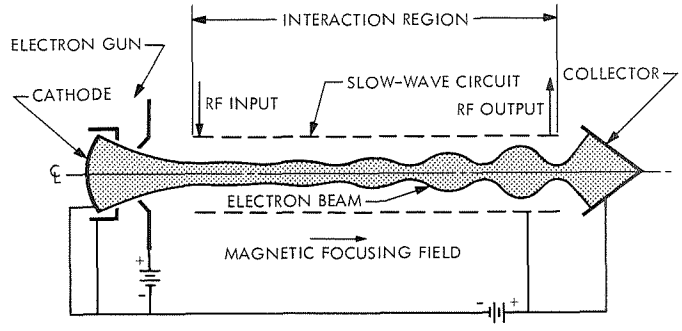

Figure 1. Schematic illustration of a traveling-wave tube

conditions are proper, the beam–wave interaction which occurs in the circuit region results in a net transfer of energy from the beam to the wave with resultant amplification of the RF signal. The increase in power carried by the circuit wave comes about as a result of a conversion of the kinetic energy of electrons in the beam. The radial circuit fields and space-charge (Coulomb) fields cause a radial perturbation of the electron trajectories during the interaction. A magnetic field is usually employed to constrain the electron beam as it passes through the circuit region; it may be a uniform axially directed field or spatially varying (e.g., periodic) field.

The performance of TWTs can be evaluated by using a nonlinear Lagrangian analysis in which the electron beam is subdivided into individual charge groups that are tracked through the interaction region. Early analyses employed a rigid-disk model for the electron beam (Reference 1). In that model, the beam is divided axially into a number of constant diameter disks of charge as illustrated in Figure 2a. The effects of radial motion of the beam electrons cannot be evaluated with such a model. Later studies (References 1 and 2) made use of a ring model in which the beam is further subdivided radially into concentric rings of charge as shown in Figure 2b. These rings were permitted to change diameter according to the radial forces acting upon them, thus accounting for the effects of radial variations. While accurate predictions of TWT performance were obtained, solutions were found to be quite costly because of the large number of charge groups required in the computer simulation. A disk model permits the use of fewer charge groups, but the modeling must be such that radial motion of the electrons and radial field variations, which have important effects in space-type TWTs, are taken into account. The "deformable-disk model" (DDM) illustrated in Figure 2c satisfies these requirements (Reference 2).

In the DDM representation of the electron beam, the disks are allowed to vary in diameter in response to the radial fields acting upon them. The radial motion of electrons contained within a disk is described

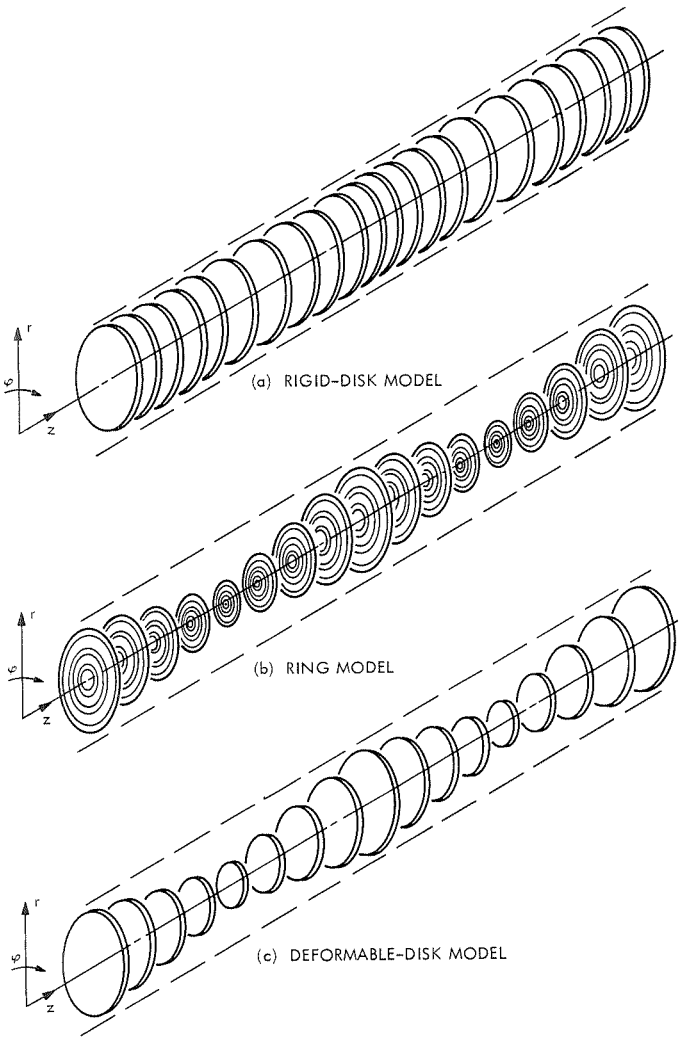

Figure 2. Electron beam models

according to laminar-flow theory. The axial motion of a disk is obtained by averaging the forces across its diameter.

Solutions to a set of nonlinear interaction equations based on the DDM representation of the electron beam, but neglecting the RF space-charge forces which result from the Coulomb interaction of the beam electrons, have been presented previously (References 2 and 3). The results show that accurate predictions are obtained for tubes in which RF space-charge forces are not the predominant factor in determining device performance. However, RF space-charge effects can be very important in the light-weight, high-efficiency traveling-wave tubes designed for space flight applications. Thus, it has been necessary to include them in the

computer calculations. Expressions for the space-charge fields, appropriate to the DDM representation of the electron beam, are presented in this article and the methods used in the calculations are described.

Expressions for the Space-Charge Fields

Explicit expressions for the space-charge fields may be obtained through the solution of Poisson's equation within the interaction region by using Green's function techniques. Rowe (Reference 1, pp. 95–97) has carried out this procedure for a ring model of the electron beam by finding the space-charge potential determined from the Green's function for a delta-function ring of charge located in a perfectly conducting drift tube. He then found expressions for the radial and axial space-charge fields by differentiating this space-charge potential function. Utilizing Rowe's results, the space-charge fields for the DDM representation of the electron beam are obtained in the following manner. The laminar-flow assumption is invoked, which permits a radial integration over all the rings of charge located at a given axial displacement plane to be performed in the ring-model space-charge-field expressions. Evaluation of the resulting equations for the radius of a disk yields the space-charge-field components at that point. The radial field component is used directly; the axial field component is averaged over the cross section of the disk.

The resulting expressions for the radial and axial space-charge-field components for the DDM representation of the electron beam are

$$E_{sc-r}(x, \Phi) = \frac{-C^2 \omega |I_0|}{u_0^2 \pi \epsilon_0 x_a^2} \int_0^{2\pi} F_{2-r}(x, x', \Phi, \Phi') \, d\Phi'_0 \tag{1}$$

and

$$E_{sc-z}(x, \Phi) = \frac{-2C^2 \omega |I_0|}{u_0^2 \pi \epsilon_0 x_a^2} \int_0^{2\pi} F_{2-z}(x, x', \Phi, \Phi') \operatorname{sgn}(\Phi - \Phi') \, d\Phi'_0 \tag{2}$$

where

$$\operatorname{sgn}(\Phi - \Phi') \triangleq \begin{cases} 1, & \text{for } \Phi > \Phi' \\ 0, & \text{for } \Phi = \Phi' \\ -1, & \text{for } \Phi < \Phi' \end{cases}$$

Table 1. Definition of symbols

a	mean radius of the circuit, m
C	gain parameter defined by $C^3 \triangleq Z_0 \lvert I_0 \rvert / 4V_0$
E_{sc-r}, E_{sc-z}	radial and axial components of the space-charge field acting on a disk of normalized radius x and phase Φ, V/m
F_{2-r}, F_{2-z}	radial- and axial-component space-charge weighting functions defined by Equations 3 and 4, respectively
I_0	dc beam current, A
$J_0(w)$	zero-order Bessel function of the first kind of argument w
$J_1(w)$	first-order Bessel function of the first kind of argument w
m	number of representative charge disks injected into the interaction region during one cycle of the RF wave
r	radial-position variable, m
u_0	average initial axial-velocity component of electrons in the beam, m/s
V_0	dc beam voltage, i.e., the dc voltage on the beam axis, V
x	normalized radius of a disk, $(C\omega/u_0)\, r$
x_a	normalized mean circuit radius, $(C\omega/u_0)\, a$
Z_0	characteristic impedance of the RF circuit (evaluated at the circuit radius) at the frequency of the wave, Ω
z	axial-distance variable, m
ϵ_0	permittivity of free space, F/m
ν_ℓ	roots of $J_0(\nu_\ell x_a) = 0$
Φ	phase position of an electron disk relative to the RF wave, rad
Φ_0	entrance phase of an electron disk, rad
ω	radian frequency of the RF wave, rad/s

The functions F_{2-r} and F_{2-z} are the space-charge weighting functions which are given by

$$F_{2-r} = \sum_{\ell=1}^{\infty} \frac{J_1(\nu_\ell x)\, J_1(\nu_\ell x')}{\nu_\ell x' \left[J_1(\nu_\ell x_a)\right]^2} \exp\left[-\nu_\ell C \left|\Phi - \Phi'\right|\right] \tag{3}$$

and

$$F_{2-z} = \sum_{\ell=1}^{\infty} \frac{J_1(\nu_\ell x)\, J_1(\nu_\ell x')}{\nu_\ell^2 x\, x' \left[J_1(\nu_\ell x_a)\right]^2} \exp\left[-\nu_\ell C \left|\Phi - \Phi'\right|\right] \tag{4}$$

where ν_ℓ is determined from the successive zeros of $J_0(\nu_\ell x_a)$, i.e., $J_0(\nu_\ell x_a) = 0$. The remaining quantities introduced in the above equations are defined in Table 1.

The space-charge weighting functions given by Equations 3 and 4 indicate the influence of a source disk of radius x' and phase Φ' on the observed disk of radius x and phase Φ. The space-charge-field components at the position of the observed disk are then evaluated by integrating over all the source disks as done in Equations 1 and 2. The radial and axial space-charge forces on the observed disk are proportional to the field components determined from these equations. This procedure can be carried out in a straightforward manner during the computer solution of the interaction equations once the radius and phase of all charge disks are known. However, the weighting functions must be evaluated many times (considering the radial and axial force on each disk due to all the disks) at each of several hundred axial displacement planes. Repeatedly evaluating them directly from Equations 3 and 4, using the actual radius and phase of each disk, would result in prohibitively long and costly computing times. Following the procedure suggested by Rowe (Reference 1) of using weighting-function tables reduces the computing time per solution appreciably and does not significantly affect the accuracy of the results.

Weighting-Function Tables

This procedure involves dividing the cross section of the interaction space into a number of annular regions (the innermost region is, of course, circular rather than annular). The weighting functions are calculated for specified values of $|\Phi - \Phi'|$ at radii corresponding to the mid-radius of each of these regions and then stored in tabular form in the computer memory. This information is used by the large-signal TWT program to evaluate the weighting functions in the manner described below, thus avoiding the need to calculate them directly so many times.

Several computer programs, separate from the DDM large-signal TWT computer program, are used to generate the weighting functions. These are used sequentially to calculate the "raw" weighting functions corresponding to the mid-radii of the space-charge regions directly from Equations 3 and 4 and then to truncate these weighting functions according to the procedure described later. The results are punched on cards which are subsequently read into the computer memory when calculations are to be made with the large-signal program. These data are in the form of tables of F_{2-r} and F_{2-z} for specified values of $|\Phi - \Phi'|$, each table corresponding to a single value of (x, x'). In the main program, the computer is instructed to scan all of the tables when particular values of x, x', Φ, and Φ' are given, select those tables (one each for F_{2-r} and F_{2-z}) corresponding to the regions within which x and x' are located, and calculate the appropriate weighting functions by interpolating (over $\Phi - \Phi'$) between the tabulated values.

It is obvious that this procedure does not yield the space-charge forces corresponding to the actual disk positions, but gives instead those forces

which would exist if each disk had a radius equal to the mid-radius of the space-charge region in which it is located. However, the resultant errors which are introduced into the calculations are not serious when a sufficient number of space-charge regions are used. This method permits a considerable reduction in computing time, which is necessary from a practical standpoint, and has given results in good agreement with experimental data. If an improvement in accuracy is desired, or required, it can be obtained by subdividing the interaction space into a larger number of space-charge regions.

Figure 3 illustrates the radial subdivision of the interaction space into seven regions, which is sufficient for most traveling-wave tubes. The values of x and x' for which the weighting functions are computed and stored are indicated in this figure, as are the radii of the space-charge-region boundaries. As mentioned previously, when looking up the weighting functions from the tables, the radius of each disk is assumed to be equal to one of these indicated values of x (or x'), regardless of its actual location within the particular region. When a disk radius crosses a region boundary, it is then assumed to be equal to the value of x (or x') for the region it has entered.

For the seven regions used in this model, there are a total of 98 weighting-function tables. Each table consists of the values of a weighting function corresponding to a single value of (x, x') at 29 distinct values of $|\Phi - \Phi'|$ which span a π range in phase. (The spacing of the $|\Phi - \Phi'|$ values was chosen as $\pi/160$ for the range 0 to $\pi/8$, $\pi/16$ for $\pi/8$ to $\pi/2$, and $\pi/4$ for $\pi/2$ to π.) Since the weighting functions are even functions of $\Phi - \Phi'$, it is only necessary to calculate and store them over a 0 to π range of $\Phi - \Phi'$ values.

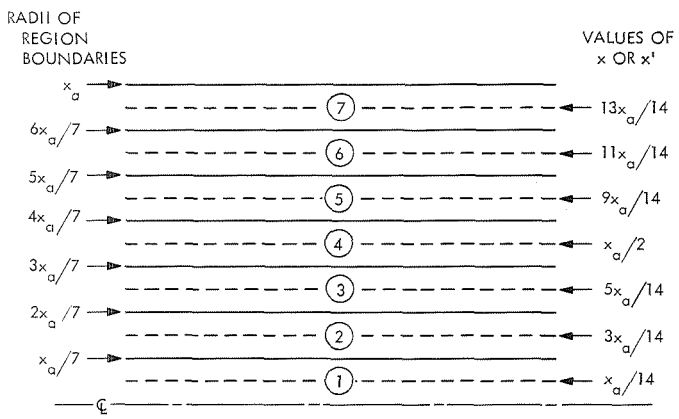

Figure 3. Division of interaction space into seven annular regions for computation of space-charge weighting functions

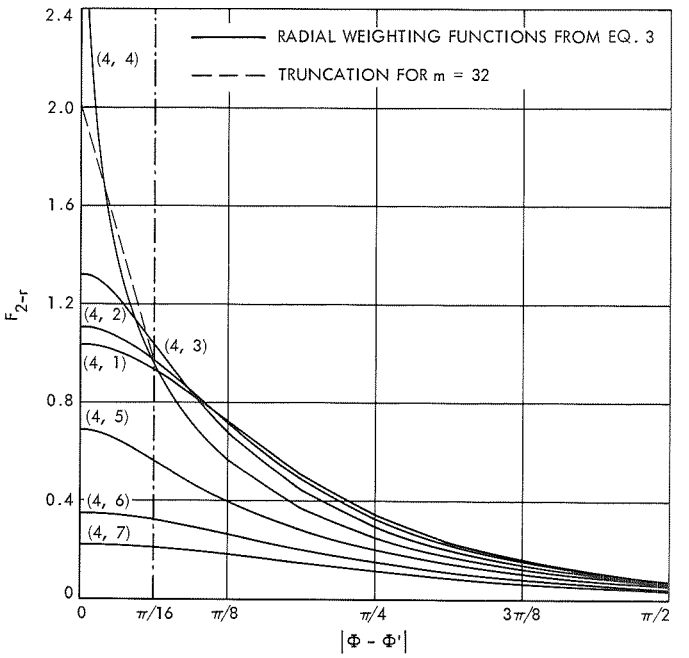

Figure 4. Radial space-charge weighting functions with $x_a/C = 1.5$, $x = x_a/2$, x' = variable

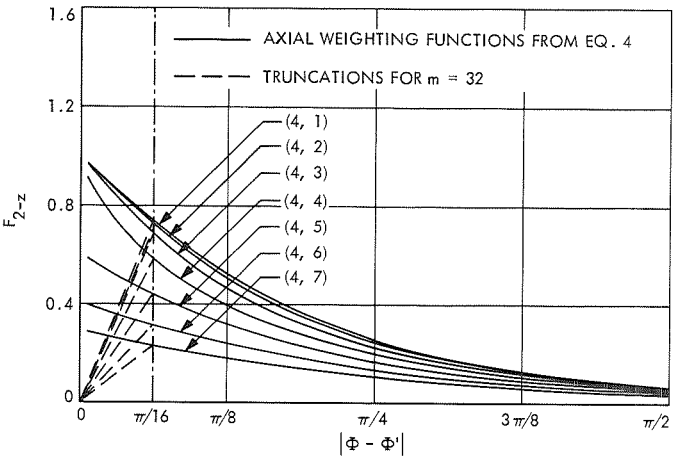

Figure 5. Axial space-charge weighting functions with $x_a/C = 1.5$, $x = x_a/2$, x' = variable

Representative radial and axial weighting functions calculated for the seven-region model using Equations 3 and 4 with $x_a/C = 1.5$ are shown by the solid curves in Figures 4 and 5. The individual weighting functions are designated by an ordered pair of numbers which correspond to the numbered space-charge regions that they represent. The first number

in a pair refers to the region in which the radius of the observed electron disk is located, while the second refers to that in which the radius of the source electron disk is located. The short-range nature of the space-charge forces is clearly indicated by these plots. As can be seen, the weighting functions are quite small at $|\Phi - \Phi'| = \pi/2$. They continue to decrease for larger phase separations and are negligibly small for $|\Phi - \Phi'| \geqq \pi$. It is this property which allows the space-charge fields to be evaluated by integrating only over a 2π phase range as done in Equations 1 and 2.

The space-charge fields calculated using the "raw" weighting functions directly are those arising from a continuous distribution of elementary charge elements, i.e., infinitesimally thin disks of charge. The discrete charge disks used in the Lagrangian analysis of the nonlinear interaction problem actually represent numerous electrons distributed over a finite volume and thus they have a finite size. The space-charge forces between these representative charge disks differ somewhat from those calculated on the basis of thin disks. However, the difference is significant only when the separation between representative charge disks becomes small enough that they, in effect, overlap. This can be taken into account approximately by truncating the weighting functions appropriately.

The method used for the axial weighting functions is to truncate them linearly to zero at $\Phi - \Phi' = 0$ from their respective values at $|\Phi - \Phi'| = 2\pi/m$, where m is the number of representative charge disks injected into the interaction region during one cycle of the RF wave. This results in a linear decrease in the axial space-charge force between two charge disks when their phase separation decreases below the initial disk spacing (which is also their effective initial phase width).

The radial weighting functions for $x = x'$ are linearly truncated from their respective values at $|\Phi - \Phi'| = 2\pi/m$ to average values at $\Phi - \Phi' = 0$ assigned according to

$$F_{2-r}(x = x')\,|_{\Phi-\Phi'=0} = \frac{m}{\pi C} \sum_{\ell=1}^{\infty} \frac{J_1(\nu_\ell x)\, J_1(\nu_\ell x')}{\nu_\ell^2 x' \,[J_1(\nu_\ell x_a)]^2} \left[1 - \exp\left(-\nu_\ell \frac{\pi C}{m}\right)\right] \tag{5}$$

This equation was derived by computing the unweighted average of F_{2-r} for $x = x'$ over the $\Phi - \Phi'$ interval from $-\pi/m$ to π/m.

The truncated weighting functions depend upon the number of charge disks per cycle of the RF wave (m) used when making the large-signal calculations. The truncations for $m = 32$ are indicated by the dashed lines in Figures 4 and 5. Although these truncation procedures certainly do not make the space-charge calculations exact, they do approximately

account for the fact that the representative charge disks are not thin disks, but instead represent a finite amount of charge distributed over a finite volume. The accuracy improves as more representative charge disks per cycle are used because they become more like the elementary charge elements for which the fields are derived and the region over which the weighting functions must be truncated is reduced. However, some sacrifice in accuracy must be accepted in order to limit the cost of the computations since the computing time increases roughly as the square of the number of charge disks employed.

Results

The accuracy of the space-charge calculations can be checked by comparing the radial forces for an unmodulated beam in Brillouin flow obtained using the weighting functions to those calculated from Gauss's law. One such calculation performed for a beam whose radius was one-half that of the circuit yielded a value of the radial space-charge force which differed from the Gauss's law value by only 1%. A computer run made with the DDM program for this case showed that the beam was perturbed by the amount expected from theoretical considerations for a 1% error in the radial space-charge force.

A number of solutions have been obtained using the DDM large-signal TWT computer program, including RF space-charge forces, for device parameters investigated previously with the TWT theory based on a ring model for the beam, a theory for which experimental verification has been obtained (Reference 2). The results were found to be in good agreement, indicating that the deformable-disk model is an adequate representation of the electron beam and that no significant errors are made in the space-charge-force calculations described here. Of particular significance is that the cost per solution using the DDM program is only about one-tenth of that required for the ring-model program.

References

1. Rowe, J. E., *Nonlinear Electron-Wave Interaction Phenomena.* Academic Press, Inc., New York, 1965.

2. Detweiler, H. K., *Characteristics of Magnetically Focused Large-Signal Traveling-Wave Amplifiers*, Technical Report 108. Electron Physics Laboratory, The University of Michigan, Ann Arbor, Oct. 1968.

3. Detweiler, H. K., and Rowe, J. E., "Electron Dynamics and Energy Conversion in O-Type Linear-Beam Devices," in *Advances in Microwaves, Vol. VI.* Academic Press, Inc., New York (to be published).